

ESTIMATES OF THE J-INTEGRAL FOR CRACKS AT REGIONS OF STRESS CONCENTRATION

*ETEMAD, M.R., DAGBASI, M., and TURNER, C.E.

Numerical results for cracks in regions of stress concentration of various geometries are presented and compared with estimates by several methods. In the LEFM regime the well known division into 'short' or 'long' crack is used. Short cracks are treated by the local stress, $(k_t \sigma)$ and a shape factor for a small crack size ratio such as $\sqrt{\pi}$, and large cracks are treated by the remote stress (σ) and a shape factor, Y , related to the size of the crack plus concentration feature. A relationship is stated to establish whether a given crack should be treated as 'long' or 'short'. In the EPFM regime the EnJ estimation method is found useful for either case provided that for cracks that are short EnJ is entered according to the local strain at the stress concentration rather than the local stress.

INTRODUCTION

Linear elastic fracture mechanics, LEFM, has proved an invaluable tool, in both design and assessment of structural integrity. It uses the crack size, a , the nominal remote stress, σ , and a geometric shape function, Y , to define the stress intensity factor, K , which gives the magnitude of the crack tip severity.

$$K = Y\sigma\sqrt{a} \quad (1)$$

To account for small scale plasticity, an estimate of the plastic zone developing ahead of the crack tip is made in conjunction with Eqn.1 to give,

$$r_p = (1/\beta\pi)(K/\sigma_y)^2 \quad (2)$$

where β is a numerical constant; 2 for plane stress (upper bound) and 6 for plane strain (lower bound). K is then increased by

*Research Assistant, Research Student and Professor of Materials, respectively; Mechanical Engineering Department, Imperial College, London SW7, UK.

replacing the crack size (a) in Eqn.1 by (a+r_p). Some users update Y correspondingly, whilst some do not. An extensive discussion on various plastic zone size estimation and correction procedures can be found in Ref.1. For more extensive plasticity, several elastic-plastic design methods have been proposed, COD(2), R-6(3), EPRI(4) and EnJ(5). These methods have been described and compared for several case studies in Ref.5.

Although most engineering structures are designed and operated within their elastic limit, they may experience yield level stresses locally at geometric discontinuities. In LEFM itself, a crack arising in a region of stress concentration is allowed for by the choice of appropriate Y factor where known, eg. Ref.5, where the Y factor is not known an approximate expression, sometimes used for short cracks is given by,

$$K = k_t \sigma \sqrt{\pi a} \quad (3)$$

Eqn.3 implies a small crack of length (a) in a remotely applied uniform stress field of magnitude k_tσ where k_t is the conventional elastic stress concentration factor evaluated here using the gross cross sectional area. In many instances, such a crack at a stress concentration is better modelled as an edge crack in a wide plate, giving,

$$K = 1.12 k_t \sigma \sqrt{\pi a} \quad (4)$$

In some of the EFPM (elastic-plastic fracture mechanics) methods the procedure for estimating the applied crack tip severity is by using an effective stress level, which at least in Ref.2 is taken as (k_tσ).

For the LEFM regime this paper presents and compares the severity of cracks in stress concentration areas as published (6), as estimated by Eqn.3, Eqn.4 and by Smith and Miller (7) and as obtained numerically. Specifically cracks emanating from elliptical holes in wide plates subjected to tensile loading with parallel ends are first studied, see Fig.1 and Table 1. The geometries modelled for the numerical studies gave rise to nominal stress concentration factors, SCF, of 2, 3 and 5. The study is then expanded to other geometries where standard solutions are not available, and the only comparison made is therefore between estimated and numerically obtained values. Analyses beyond LEFM regime is then detailed by comparing computed J-integral values with those predicted by EnJ, for both short crack and long crack cases. The local plastic strain in the notch, as found by finite element study of the uncracked body, was also used in the EnJ estimation procedure.

TABLE 1 - Details of Geometries Studied.

(a) Elliptical centre notch (Fig.1.a)

Case	W mm	D mm	R mm	H mm	SCF	
					Nominal	True
M212	100	100	5	10	2	2.04
M202	50	200	5	10	2	2.041
M203	50	200	10	10	3	3.153
M205	50	200	10	5	5	5.183

(b) Edge notch tension (Fig.1.b)

Case	W mm	D mm	R mm	H mm	Type of Notch	SCF
M202T	50	200	5	10	Semi-elliptical	2.124
M205T	50	200	10	5	Semi-elliptical	5.869
M99RT	10	40	1.8	0.5	u-notch	7.8

(c) Edge notch bending (Fig.1.c)

Case	W(mm)	D(mm)	R(mm)	H(mm)	Type of Notch	SCF
M202B	50	200	5	10	Semi-elliptical	1.627
M205B	50	200	10	5	Semi-elliptical	4.475
M99RA	10	40	1.8	0.5	u-notch	5.5
M99R	10	40	2	0.5	u-notch	5.8

(d) The structure (Fig.1.d, 1.e)

Case	W(mm)	D(mm)	R (mm)	H (mm)	Loading	SCF
M121B	50	200	5	10	Bending	1.465(1.187)
M121T	"	"	"	"	Tension	1.55(1.400)*

*Figures in parenthesis are based on reduced section area.

THE FINITE ELEMENT PROGRAM

A two-dimensional, small geometry change FE code with 8 noded isoparametric elements was used to model various structures for numerical study. The material modelled was a pressure vessel steel with mild work hardening with yield stress $\sigma_y = 573.64 \text{ MN/m}^2$. Young's modulus $E = 210 \times 10^3 \text{ MN/M}^2$, and Poisson's ratio $\nu = 0.3$.

All geometries studied were constrained to plane strain, and the J-integral was evaluated along 10 different contours around the crack tip, to prove path independence of the method. Whilst elastic, these values were converted to K and Y using

$$K = \sqrt{J/E'} = Y\sigma\sqrt{a_t} \quad (5)$$

$$\text{where } E' = E/(1-\nu^2) \quad \text{and} \quad (6a)$$

$$a_t = a + R \quad (6b)$$

where R is the notch size (see Fig.1).

STRESS CONCENTRATION CASES IN LEFM

Infinite Geometry Cases

Estimates of the stress intensity factor K by Eqns 3 and 4 and those obtained using the equations given by Smith and Miller (7), are compared with FE results obtained here and those presented in Ref.6, for cracks at elliptical holes in three cases of nominal SCF, 2, 3 and 5, in Fig.2. Note that the geometries studied by the FE method were of finite size, see Fig.1a and Table 1a, so that a correction to infinite size was made using $\sqrt{\sec(\pi a_t/w)}$ due to Feddersen (8). The FE results agree with those given in Ref.(6) being 2% higher, but predictions by Eqn.3 are always lower for low SCF cases. For higher SCF cases predictions by Eqn.3 are lower for small cracks and higher for longer cracks than those given by Ref.6. On the other hand Eqn.4 predicts exact or higher K values for all those cases presented in Fig.2. The amount of over-estimate by Eqn.4 depends upon both the crack size (a) and the SCF. For

short cracks the prediction by Eqn.4 approaches to the exact solution. Fig.2 further shows that the stress intensity factor for these geometries increases with the increase of crack size, approaching to the centre crack panel solution after slightly overshooting it. Therefore, the stress intensity factor predicted by the long crack (a_t) approach, that is the centre crack panel with a crack size ($2a_t$), using Eqn.7, which is essentially Eqn.5 with $Y=\sqrt{\pi}$, while being reasonably accurate for long cracks, will be perhaps too conservative for short cracks.

$$K = \sigma\sqrt{\pi a_t} = \sigma\sqrt{\pi(a+R)} \quad (7)$$

Furthermore use of Eqn.4 for short cracks proves to be a good or slightly conservative estimate of the true stress intensity factor. A simple criterion to distinguish those cracks in a region of stress concentration where a short crack approach will be better than the long crack approach and vice versa can be obtained by equating the two solutions for K, i.e. Eqns.4 and 7, for a particular crack length a' .

$$K = k_t \sigma 1.12\sqrt{\pi a'} = \sigma\sqrt{\pi a_t} = \sigma\sqrt{\pi(a'+R)} \quad (8)$$

to give,

$$a' = R / |(1.12k_t)^2 - 1| \quad (9)$$

if $a < a'$ a short crack treatment (Eqn.4) is preferred

$a > a'$ a long crack treatment (Eqn.7) is preferred.

Finite geometries

The idea of a 'short crack' in an elevated tensile stress field ($k_t\sigma$) or 'long crack' in the stress field (σ) can be extended to cover edge notch cases in geometries of finite sizes, such as parallel end tension and bending. To apply to such cases, Eqns.4 and 7 are modified for finite sizes, respectively, as follows.

$$K = k_t \sigma Y_S \sqrt{a} \quad (10a)$$

$$K = \sigma Y_L \sqrt{a+R} \quad (10b)$$

Equating these, for a particular crack length, gives,

$$a' = R / |k_t Y_S / Y_L|^2 - 1| \quad (11)$$

where

$Y_S = Y_S(a, W_n, D)$ as is taken in tension

$Y_L = Y_L(a_t, W, D)$ as is taken for the actual geometry (see Fig.1.a,b,c,d,e).

FRACTURE CONTROL OF ENGINEERING STRUCTURES – ECF 6

Use of Eqn.11 enables a decision to be made on the 'short crack' or 'long crack' treatment of a crack problem in a stress concentration area. Again when $a < a'$ the short crack treatment is preferred and for $a > a'$ the long crack treatment is preferred.

A summary is given in Table 2, comparing long or short crack treatments for those geometries studied, see Table 1 and Fig.1, to support the criteria stated above. Where relevant estimates using the equations given by Smith and Miller (Ref.7) are also given

TABLE 2 - Comparison of Estimated and Numerically obtained Stress Intensity Factors

(a) Cases favouring short crack approach

Case	SCF	a' + (mm)	a (mm)	K/σ ⁺		
				Computed	Eqn.10a	Eqn.10b
M202T	2.12	1.71(1.3) ⁺	0.5	2.83	2.98(2.75)	4.99
"	"	1.71(1.3)	1.0	3.8	4.25(3.90)	5.17
"	"	1.71(1.3)	1.5	4.47	5.16	5.43
M202B	1.63	2.035	0.5	2.32	2.28	4.07
M121T	1.55	4.52	2.5	4.27	5.04	5.92
M121T(*)	1.4	5.21	2.5	3.92	4.71	3.36
M121T(*)	1.4	5.21	5.0	5.41	6.60	4.72
M121B(*)	1.19	4.27	2.5	3.12	3.86	2.85

(b) Cases favouring long crack approach

Case	SCF	a' (mm)	a (mm)	K/σ ⁺		
				Computed	Eqn.10a	Eqn.10b
M205T	5.87	0.39(0.65)	0.5	5.98	8.24(5.07)	7.35
M205B	4.48	0.4	0.5	4.58	6.28	5.65
M99RA	5.5	0.05	0.2	2.44	3.67	2.45
M99R	5.8	0.05	0.1	2.33	3.64	2.53
"	"	"	0.2	2.58	5.15	2.60
"	"	"	0.25	2.66	5.76	2.63
M99RT	7.8	0.04	0.2	3.16	7.42	3.18
M121T	1.55	4.52	5.0	6.01	7.31	7.12
M121B	1.47	2.43	2.5	3.91	4.76	4.72
M121B	"	"	5.0	5.08	6.97	5.50
M121B(*)	1.19	4.27	5.0	4.11	5.65	3.92

+ Figures in parenthesis are obtained using Ref.7.

* Stress is based on the reduced section area ie. R=0 in Eqn. 10b.

THE COMPUTED RESULTS AND EnJ

Given the material properties, σ_y , E, and a limiting value of J, $J=J_c$, estimates of J can be converted to either:

- i) an allowable stress level if crack size and shape factor Y are known, or
- ii) an allowable crack size if stress level and shape factor Y are known.

Here the data are examined according to EnJ, although remarks similar in nature but differing considerably in detail could also be made in respect to COD(2), R-6(3) and EPRI(4).

The EnJ equations (9) are

$$J/G = (e_f/e_y)^2 |1 + 0.5(e_f/e_y)| \quad \text{for } e_f/e_y \leq 1.2 \quad (12a)$$

$$J/G_y = 2.5 |e_f/e_y - 0.2| \quad \text{for } e_f/e_y > 1.2 \quad (12b)$$

where (e_f/e_y) is the effective strain ratio and G_y is the LEFM value of $G(=K^2/E)$ with $\sigma=\sigma_y$.

In the near LEFM regime, while yield is still contained near the crack tip region, the remotely applied stress ratio (σ/σ_y) may be used instead of e_f/e_y . This near LEFM regime is defined in Ref.10 as:

$$Q/Q_f \leq 0.8 \quad (13)$$

where $Q =$ Applied load or moment

$$Q_f = B.b.\sigma_y \quad \text{for tension} \quad (14)$$

and $Q_f = (B.b^2.\sigma_y)/4$ for bending (15)

Comparison of Data with EnJ

J/G_y obtained from Eqn.12, based on (σ/σ_y) , will depend upon the applied load only. This is shown in Fig.3 where it is compared with data from numerical studies using the correct shape factor as obtained from computation. For load levels $Q/Q_f \leq 0.8$, EnJ predictions are either exact or upper bound to numerical results for all geometries studied here. These correspond to a stress level of $\sigma/\sigma_y \leq 0.72$ in tension and $\sigma/\sigma_y < 1.08$ in bending in the present cases where both a/w and a_t/w_y are small. As can be seen the EnJ predictions are a good estimate of the true J/G_y for small cracks in a low stress concentration region, but a margin of conservatism extends as either the crack size or SCF is increased. Examining Table 1 together with Fig.3 shows that the smaller the (K/σ) obtained from a small crack treatment (Eqn.4) as compared to that

obtained from a large crack treatment, Eqn.7, the closer the estimate by EnJ is to the numerical result.

Estimation by EnJ

In the EnJ estimation method, "the short crack" approach is implemented by entering Eqn.12 at $(k_t \sigma / \sigma_y)$ and using the actual crack size (a) together with a shape factor $Y = Y_t(a, w)$, see Fig.1. On the other hand "the long crack" approach is implemented by entering Eqn.12 at remote stress levels (σ / σ_y) , and using $(a_t = a + R)$ for the crack size together with a shape factor $Y = Y_l$ appropriate for the geometry and (a_t / w) . Note that for the geometries studied in the short crack treatment the shape factor Y_t is approximated to $1.12\sqrt{\pi}$, since $a/w \leq 0.1$, and in the "long crack" treatment, since $a_t/w \leq 0.28$, the shape factor Y_l is approximated to $\sqrt{\pi}$ for center crack and $1.12\sqrt{\pi}$ for edge crack.

In Fig.4, the shortest cracks for all cases studied here are shown as treated by the short crack approximation, irrespective of 'long' or 'short crack' analysis required according to Eqn.11. Clearly the EnJ estimation for those cases requiring long crack analysis becomes too conservative, e.g. M205 and M99R. In Fig.5, the data is shown again treated by the 'long crack' crack analysis. Here the EnJ estimation procedure for cases requiring short crack analysis becomes too conservative, e.g. M202B. Moreover, if allowable crack sizes (in this case $a_t = a + R$) are to be evaluated for a given applied load, it is very likely that one will end up with a crack size a_t which is actually shorter than the notch size R . It is therefore concluded that the division between the long and short crack treatments in the LEFM regime must be carried over into contained yielding.

Contained Yielding and beyond

A better approach, also consistent with the EnJ derivation, is to use the effective strain ratio (e_f / e_y) . For short cracks the notch tip strain, NTS, ratio (e_T / e_y) in the absence of any crack, may be used in EnJ equations. For rigorous LEFM $(e_T / e_y) = k_t (\sigma / \sigma_y)$, but with any degree of yielding these terms differ. Estimates from EnJ by using the NTS ratio (e_T / e_y) obtained by computation, are compared with the numerical results in Fig.6. The agreement of EnJ for short cracks obtained in this way appears to have improved for those cases strongly favouring short crack treatment. Therefore, true notch tip strain ratio entered into EnJ gives a good estimate, both in LEFM and in contained yielding, for cracks in stress concentration area, favouring 'short crack' treatment. Hence future work includes estimating the NTS in a stress concentration area in the absence of any crack. Neuber (11) type analysis as suggested by Begley et al (12) is favoured for this study and extension to yet more extensive yielding is envisaged.

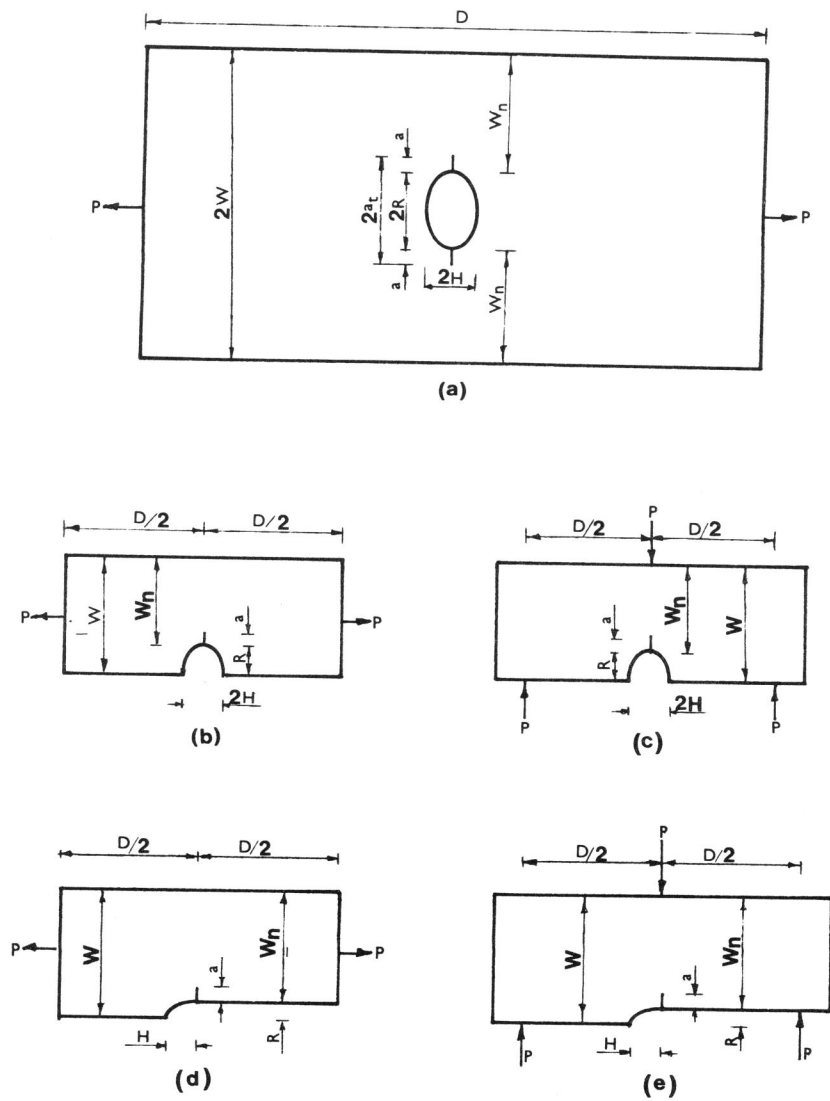
CONCLUSIONS

A simple formulation has been proposed dividing a "short crack" from a "long crack" treatment for cracks at regions of stress concentration. Comparison of computed data all with $SCF \leq 5$ and with $a/W \leq 0.28$, with exact solution support the analysis which is then carried over into other configurations for which exact solutions do not exist. This same concept is applied to cases with some degree of yielding and good agreement found with estimation by EnJ when entered at the local strain e_t/e_y in the uncracked body.

REFERENCES

- (1) Turner, C.E., Methods for post yield fracture mechanics, "Post Yield Fracture Mechanics", Ed. D.G.H.Latzko, App.Science Pub., 1979, Ch.2.
- (2) Guidance of Some Methods for The Derivation of Acceptance Levels of Defects in Fusion Welded Joints, British Standards Institution, PD6493, 1980.
- (3) Harrison, R.P., Loosemore, K., and Milne, I., Assessment of the integrity of structures containing defects, CEBG Report R/H/R6, 1976 and supplements 1979, 1981.
- (4) EPRI Ductile Fracture Research Review Document, Ed. O.M.Norris et al., EPRI, (Palo Alto), Dec.1980.
- (5) Turner, C.E., ASTM STP 803, Vol.II, 1983, pp.80-102.
- (6) Rooke, D.P., and Cartwright, D.J., "Compendium of Stress Intensity Factors", Her Majesty's Stationery Office, London, 1974.
- (7) Smith, R.A., Miller, K.J., Int.J.Mech.Sci., Vol.20, year, pp.201-206.
- (8) Feddersen, C.E., Discussion, ASTM STP 410, 1967, pp.77-79.
- (9) Turner, C.E., The J-Based Fracture Assessment Method, EnJ , and Application to Two Structural Details, ICF6, Vol.2, pp.1053-1061.
- (10) Turner, C.E., A J-Based Engineering procedure (EnJ) for fracture safety assessment. Seminar sponsored by 'H.M. Nuclear Installation Inspectorate', M.P.A. Stuttgart, Oct.1982.

- (11) Neuber, H., Transactions of ASME, 1961, pp.544-550.
- (12) Begley, J.A., Landes, J.D., and Wilson, W.K., ASTM STP 560, pp.155-169.



(a) Center notch tension
 (b,c) Edge notch tension and bending
 (d,e) Structure in tension and bending

Figure 1, Details of geometries studied

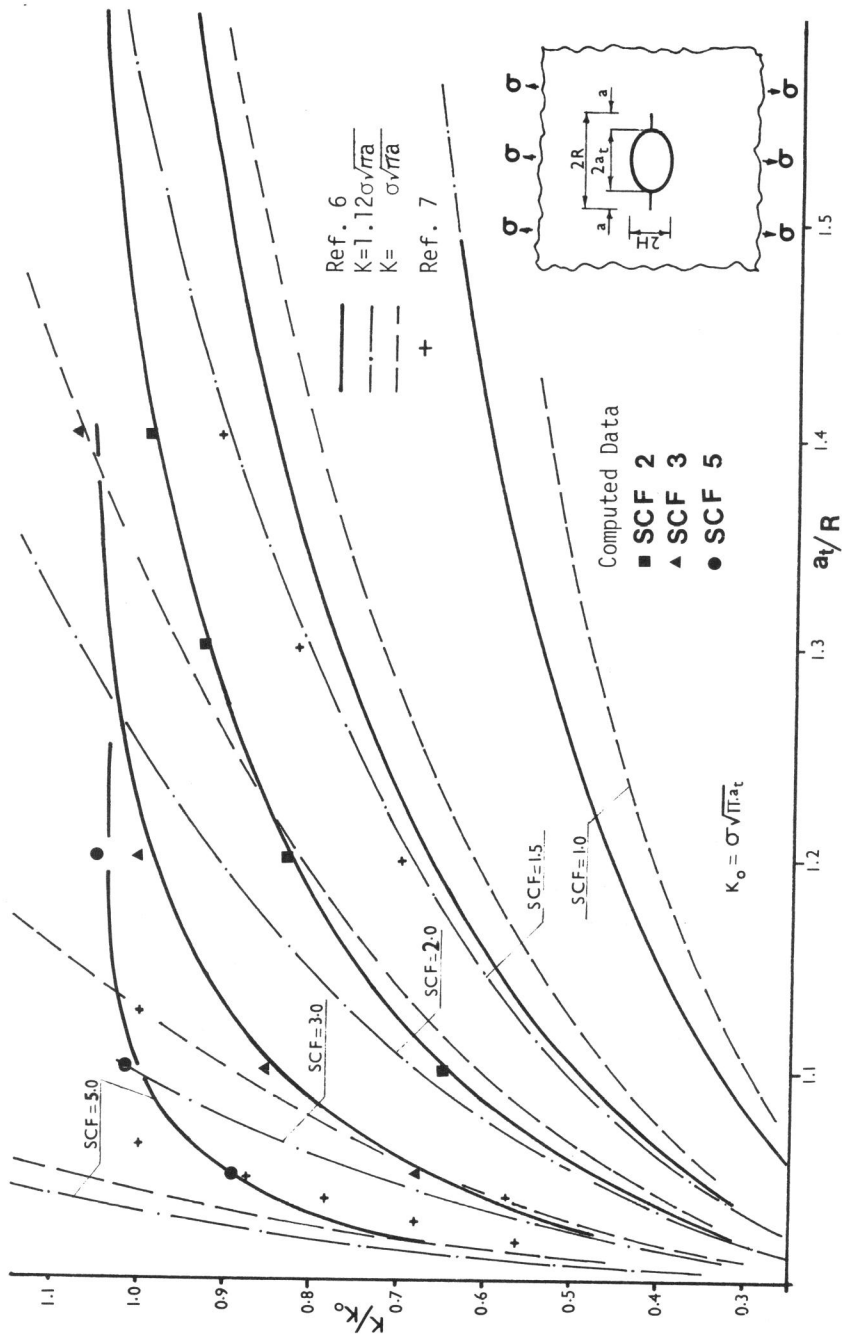
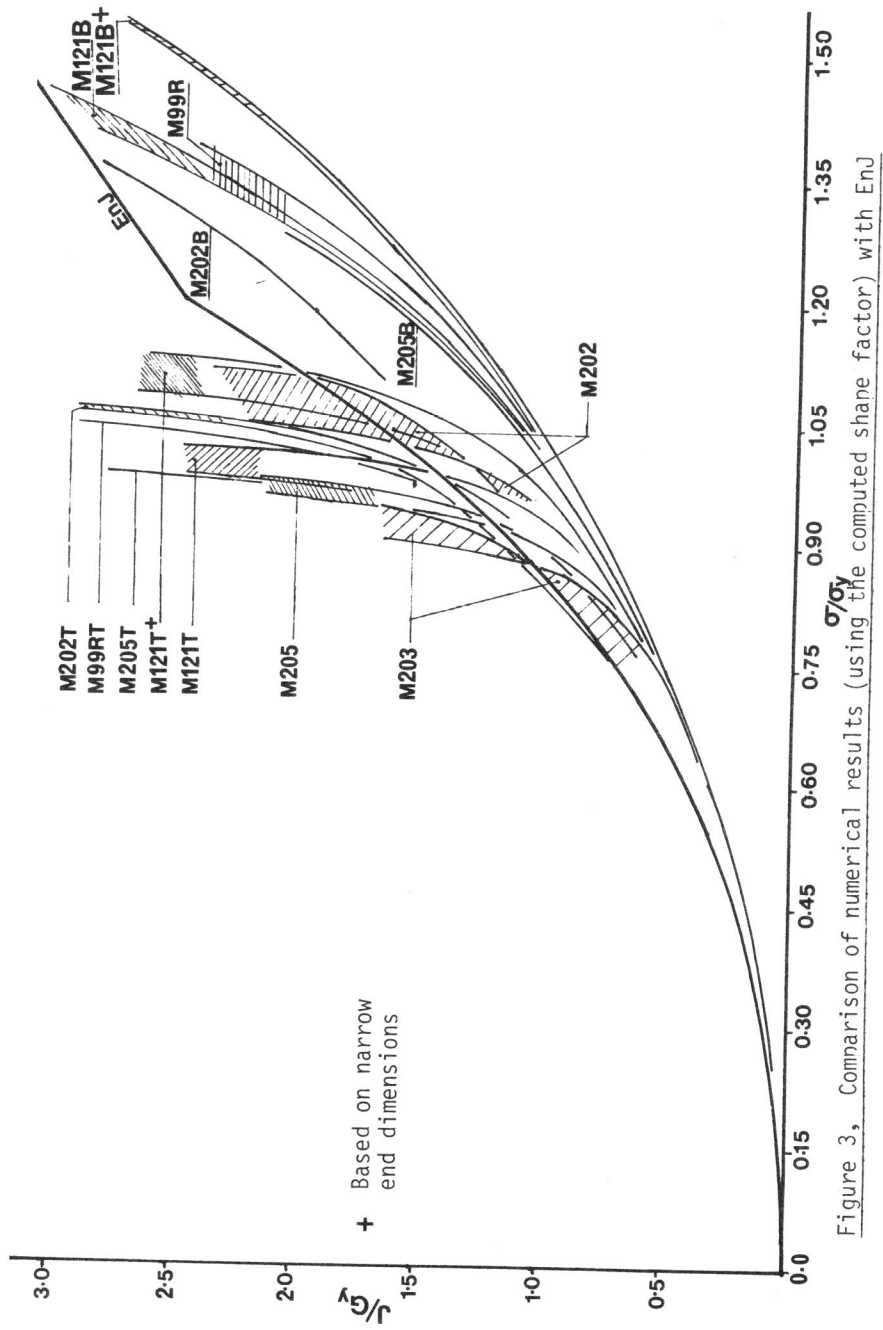


Figure 2, Comparison of stress intensity factors for infinite plates



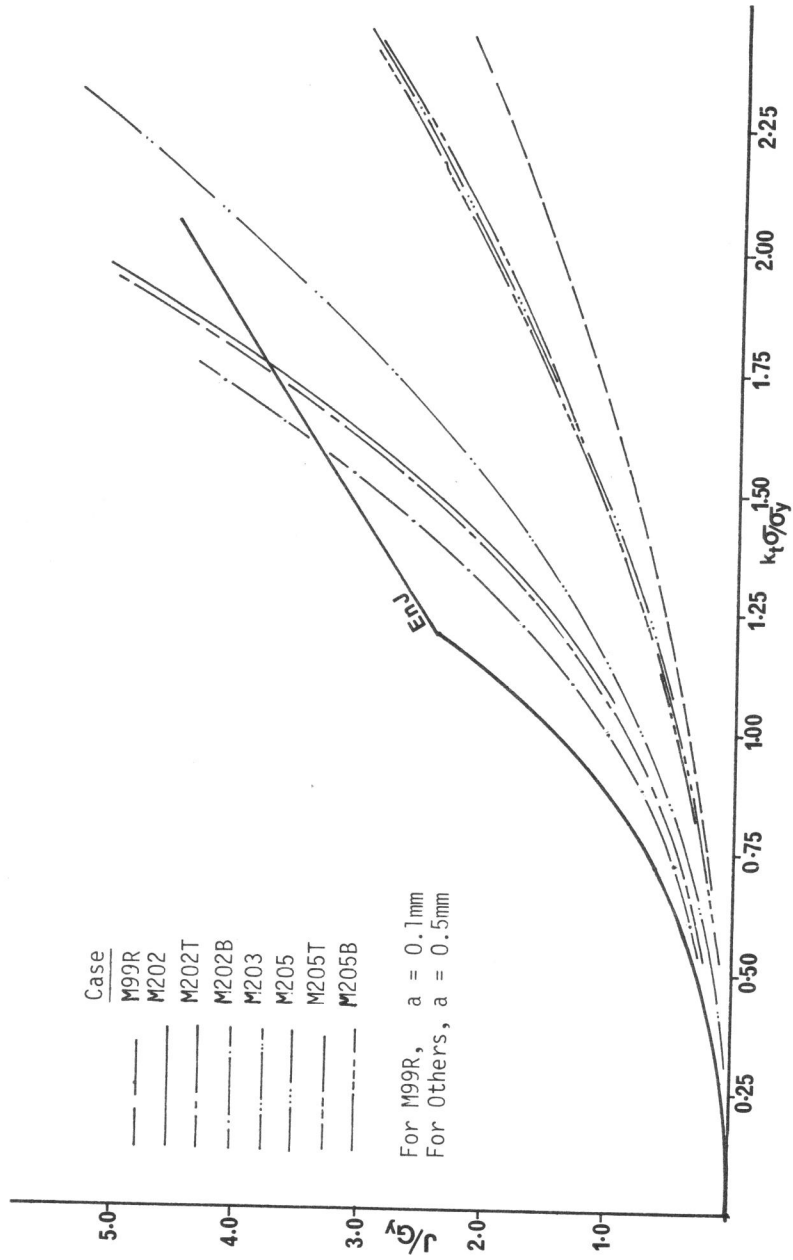


Figure 4, 'Short Crack', (a) treatment of numerical data using $Y=1.12\sqrt{\pi}$ and comparison with EnJ entered at $(k_t \sigma / \sigma_y)$

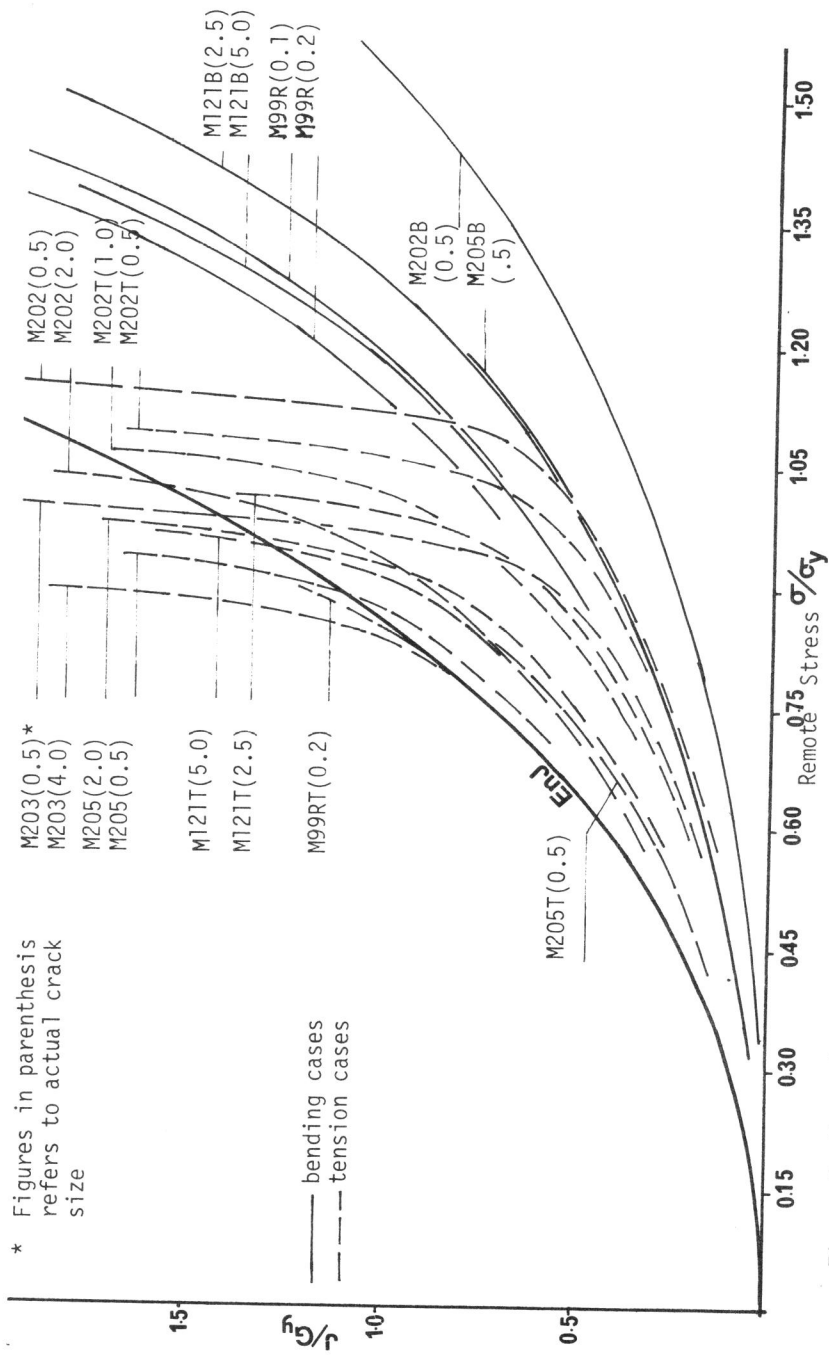
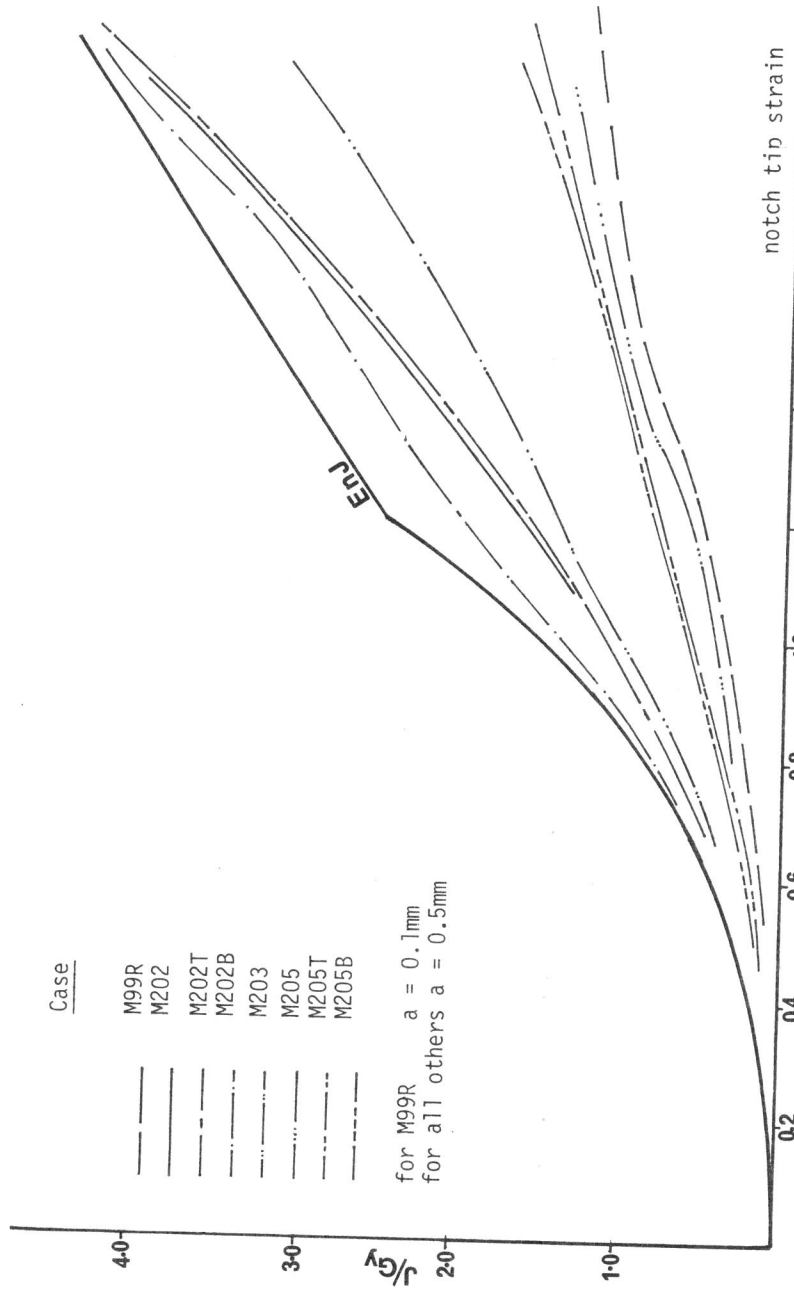


Figure 5, 'Long Crack', (a) treatment of numerical data using $y=\sqrt{r}$ ($1.12\sqrt{r}$ for edge crack geometries) and comparison with ENJ entered at (σ/σ_y) .



Case

- M99R
- M202
- M202T
- M202B
- M203
- M205
- M205T
- M205B

for M99R $a = 0.1\text{mm}$
for all others $a = 0.5\text{mm}$

Figure 6. 'Short Crack' (a) treatment of numerical data with $\gamma = 1.12\sqrt{r}$ and comparison with ENJ entered at true notch tip strain.